1.7 Joining of 14YWT and F82H by Friction Stir Welding — D. T. Hoelzer, M. A. Sokolov and Z. Feng, ORNL

OBJECTIVE

The objective of this work was to investigate the feasibility of joining specimens of the advanced ODS 14YWT alloy with each other and with F82H by friction stir welding.

SUMMARY

A sample was prepared for the initial joining study using friction stir welding (FSW) that consisted of 4 specimens of the advanced oxide dispersion strengthened (ODS) 14YWT-SM6 ferritic alloy, 15 mm long, 6 mm wide and 2.86 mm thick each, that were spot welded in a corresponding slot that was machined in an F82H plate. The FSW run was successfully performed on the sample using a polycrystalline boron nitride tool (PCBN) that resulted in joints showing good bonding between specimens of 14YWT-SM6 and between 14YWT-SM6 and F82H. The joints were characterized by light microscopy and SEM analysis and were observed to be relatively narrow in width. However, porosity was observed in the thermomechanically affected zone (TMAZ) of 14YWT-SM6 on the advancing side of the FSW joint and at the interface between F82H and 14YWT-SM6. Further refinements in the FSW process will be required to minimize defects including porosity.

PROGRESS AND STATUS

Introduction

Friction stir welding (FSW) is an innovative solid-state joining technique that was invented in 1991 [1]. The basic concept of FSW involves plunging a specially designed tool rotating at high speeds into the seam between work pieces and joins them by solid-state mixing as the tool travels along the seam. Heat is produced by friction from contact between the rotating tool and work pieces that allows material to flow around the tool during the translation of the rotating tool. As the tool travels along the seam to be joined, a cavity forms at the rear but is filled with material redistributed by the rotating tool to form the weld. The redistribution process causes the material to experiences extreme levels of plastic deformation and thermal exposure that can have a significant effect on microstructural changes in weld zone. A recent review of the friction stir welding and related friction stir processing methods has been published [2].

The FSW technique was originally developed for the Al industry. However, since the FSW technique is based on the solid state joining concept, it has recently been applied to joining high performance alloys that typically are produced with complex microstructures. Oxide dispersion strengthened (ODS) ferritic alloys (FA; >12Cr) and tempered martensitic steels (TMS; <12Cr with C) represent a class of complex high performance materials that are produced by the mechanical alloying method to utilize a dispersion of thermally stable oxide particles to greatly improve the strength and creep properties at elevated temperatures. Although there have been a limited number of FSW studies that have been conducted on ODS alloys in the recent past, these studies demonstrated that joints could be produced with INCO MA957 FA [3,4], INCO MA956 [5,6], ODS Eurofer 97 TMS [7] and Plansee PM2000 FA [8]. However, further research focusing on improvements in the FSW conditions and microstructural characterization is needed in order to improve the joints that are produced in ODS FA and TMS.

Recent advances in understanding the MA process have led to development of the advanced ODS 14YWT ferritic alloy, or Nanostructured Ferritic Alloy (NFA), during the past 10 years. The salient characteristics of 14YWT consist of a high number density of 2-4 nm dia. Ti-, Y-, and O-enriched particles, or nanoclusters (NC), and nano-size (<500 nm) grains that provide high strength up to 800ºC [9]. Numerous small heats of 14YWT have been produced with similar NC dispersion and grain size characteristics. The purpose of this study was to investigate the feasibility of joining specimens of 14YWT by FSW without degrading the highly tailored microstructure. In addition, the study also focused on joining dissimilar materials of 14YWT to F82H. The 14YWT used in this study was from the 14YWT-SM6 heat that was produced in 2005. This heat was primarily used in the doctoral research project of McClintock [10]. The objective of this project was to investigate the tensile and fracture toughness properties of 14YWT-SM6 before and after exposure to neutron irradiation at HFIR to a dose of ~1.35 dpa at 300ºC. A significant highlight obtained in this study was the discovery that the 14YWT-SM6 heat possessed a fracture toughness transition temperature of -150ºC and upper shelf energy of ~150-175 MPa·m$^{0.5}$ that did not change after neutron irradiation [11, 12].

Procedure

The specimens used in the friction stir welding experiments were prepared from material of 14YWT, 14WT and F82H. The 14YWT was from the SM6 heat that was produced in 2005. The nominal composition of the 14YWT-SM6 heat was Fe-14Cr-3W-0.4Ti + 0.3Y_2O_3 (all values in wt. %). The 14WT was from the SM3 heat that was also produced in 2005. The 14WT-SM3 heat was a reference heat to 14YWT-SM6 since it was ball milled with no Y_2O_3, so the nominal composition was similar to 14YWT-SM6 but contained no Y. It was planned to use the 14WT specimens in the trial FSW attempt to help elucidate any changes in the FSW parameters that may be required to make before attempting the experiment with the 14YWT-SM6 specimens. Both the 14YWT-SM6 and 14WT-SM3 heats were 0.8 kg in mass and were processed with similar conditions, i.e. ball milling time of 40 h and extruded at 850ºC. The F82H plate used in this experiment was supplied to ORNL by JAEA.

A total of 4 specimens were produced from the 14TYWT-SM6 and 14WT-SM3 heats. These specimens were cut from the end of broken dual notch bend bar specimens that were used in three point bend tests in the unirradiated condition. A dual notch bend bar specimen that was fabricated from 14YWT-SM6 prior to the three point bend test is shown in Figure 1. The fracture surfaces of the tested specimens were preserved.

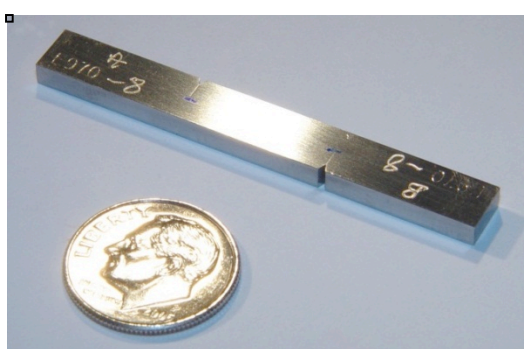

Figure 1. A dual notch bend bar specimen that was used to prepare specimens of 14YWT and 14WT to be used in the friction stir welding experiment.

The preparation of 2 samples used in the FSW study consisted of embedding 4 specimens of the NFA 14YWT and the reference 14WT (ball milled with no Y_2O_3) within several plates of F82H. First, a 12 x 30 mm^2 slot was cut by Electro Discharge Machining (EDM) in a plate of F82H that was 63 mm long, 25 mm wide and 2.86 mm thick. A total of 4 specimens of 14YWT and 14WT were cut from the ends of dual notch bend bar specimens that had been tested. The dimensions of these specimens were 15 mm long, 6 mm wide and 2.86 mm thick. The 4 specimens were then arranged in the 12 x 30 mm^2 slot that was cut from the F82H plate. Next, a 30 mm long, 25 mm wide and 2.86 mm plate of F82H was placed next to the plate containing the slot holding the 4 specimens of 14YWT and 14WT in place. Two additional plates of F82H possessing the same dimensions described previously were used as backing plates. Finally, spot welds were used on butt joints holding the 14YWT and 14WT specimens in the slotted F82H plate and between the plates of F82H as shown in Figure 2. For both samples, the extrusion direction of the 14YWT-SM6 and 14WT-SM3 specimens lies parallel to the long axis of the bend bar specimens. Therefore, the traveling direction of the rotating tool during FSW was parallel to the extrusion direction of these specimens, i.e. from left to right in Figure 2.

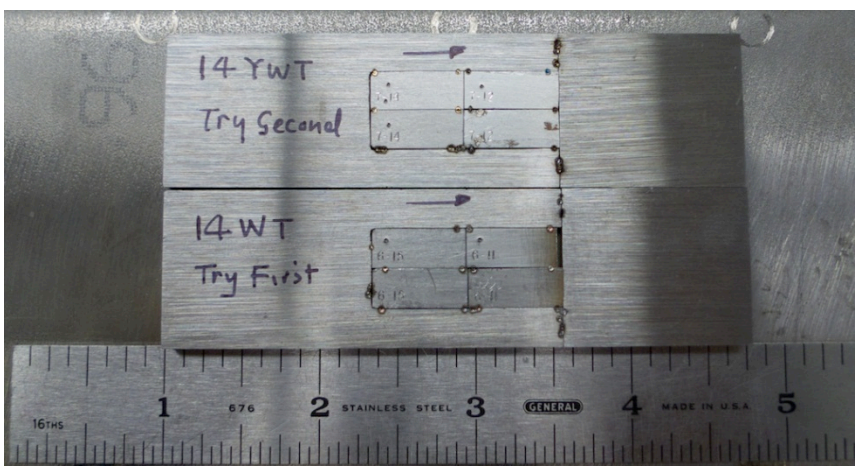

Figure 2. Digital image showing the 4 spot welded specimens of 14YWT-SM6 and 14WT-SM3 embedded in the slots that were cut in the F82H plates.

Operation of three independent axes with adjustable, adaptable pin tools for on-the-fly mode switching between fixed, adjustable, and self-reacting welding modes. It can also handle computer controlled operation and key process parameter monitoring and is capable of making non-linear, variable-thickness, and double-curvature welds. The friction stir welding experiments were conducted using a pin tool fabricated from Polycrystalline Cubic Boron Nitride (PCBN). After the FSW runs were performed on the 2 samples, 3 specimens were cut from the FSW zones and mounted and polished for microstructural characterization. The location of the 3 specimens is shown in Figure 3. One specimen was cut at the leading edge of the bend bar fracture toughness specimens and the next 2 specimens were cut at the 0.25L (L = 30 mm) and 0.50L positions.

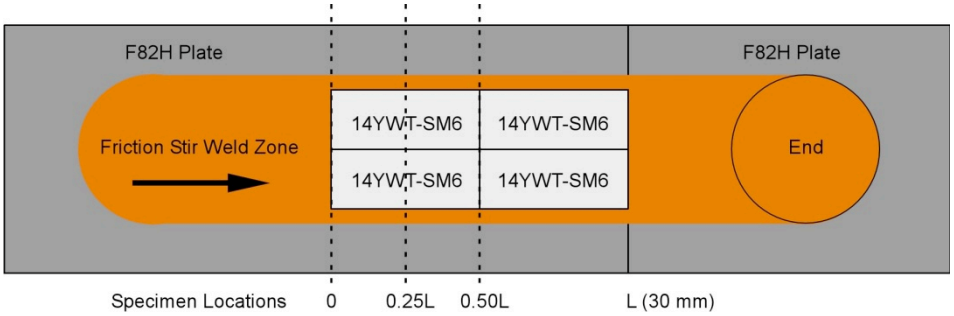

Figure 3. Schematic showing the location of specimens cut from the FSW zone and mounted for metallography and SEM analysis.

RESULTS AND DISCUSSION

Friction Stir Welding Experiment

The initial FSW run was performed on the 14WT-SM3/F82H sample and was then followed by the FSW run on the 14YWT-SM6/F82H sample. Digital images depicting the friction stir welding process on the 2 samples is shown in Figure 4. The PCBN tool making initial contact with the 14WT-SM3/F82H sample to start the joining process is shown in Figure 4a. The completed FSW runs that were performed on both samples are shown in Figure 4b. The results show that mixing by FSW occurred over areas in both samples that included material from the F82H plate and the bend bar fracture toughness specimens of 14WT-SM3 and 14YWT-SM6, as was shown in Figure 2. In addition, it should be pointed out that the PCBN pin tool did not fracture during each of the 2 FSW runs.

(a)

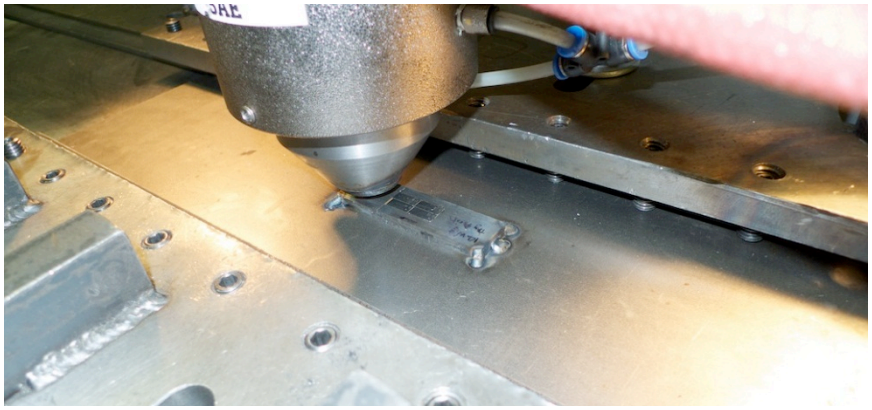

(b)

Figure 4. Digital images showing (a) contract between PCBN tool and the initial 14WT-SM3/F82H sample and (b) the completed friction stir welds of the 14WT-SM3/F82H and 14YWT-SM6/F82H samples.

Microstructural Characterization

The preliminary microstructural study of the F82H/14YWT-SM6 sample was conducted on the specimen that was cut at the 0.25L location. The microstructure of the specimen viewed in cross section by light microscopy is shown in Figure 5. This specimen was polished and etched to reveal the F82H plate located on the bottom and right side. The chemical etch had little effect on 14YWT-SM6, which appears mostly shiny due to the high (14%Cr) content combined with the nano-size grain structure. Etching was able to reveal the interface between the

thermomechanically affected zone (TMAZ) and heat affected zone (HAZ) on the advancing side of the FSW joint of 14YWT-SM6. However, no discernable interfaces were observed near the center of the weld nugget between 2 bend bar specimens of 14YWT-SM6 or on the retreating side of the FSW joint. An interface was observed between the TMAZ of the F82H plate and 14YWT-SM6 specimens. These results indicated that good bonding occurred between the bend bar specimens of 14YWT-SM6 and between F82H and 14YWT-SM6 in the initial FSW attempt. On the other hand, several large pores were present in the lower side of the TMAZ of 14YWT-SM6 on the advancing side, which indicated that the FSW process conditions still need to be refined.

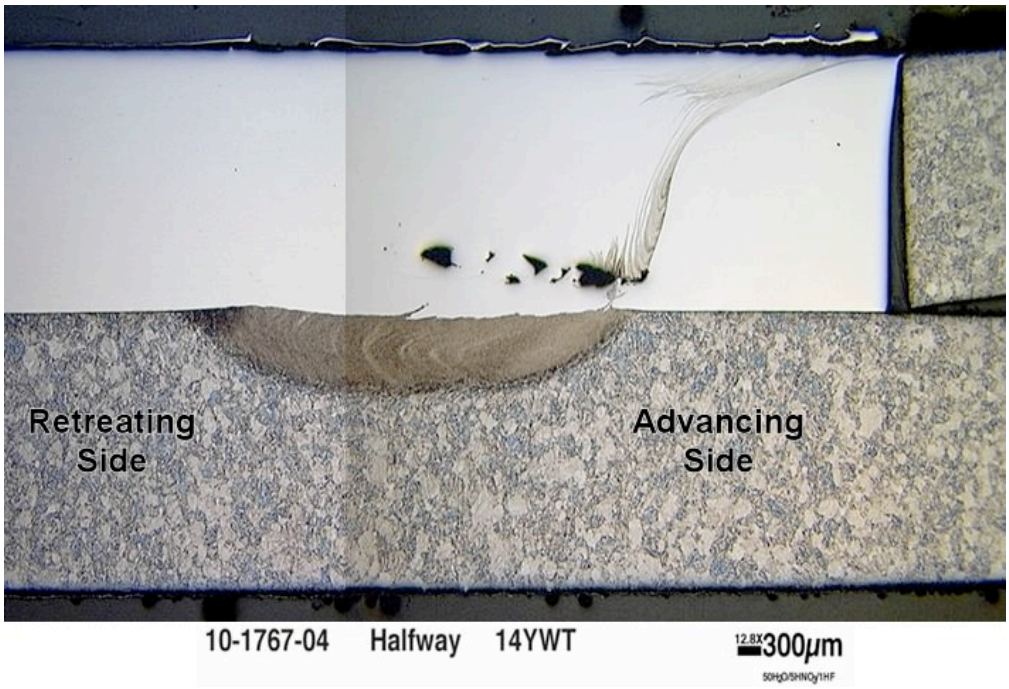

Figure 5. Light micrograph showing the cross sectional view of the FSW joint located at the 0.25L (L=30 mm) position.

SEM analysis was performed on the same specimen (0.25L) of the F82H/14YWT-SM6 sample that was shown in Figure 5. However, the mounted specimen was re-polished, with a final polish using colloidal silica and no subsequent etching. This procedure was required in order to image the nano-size grains present in 14YWT-SM6 using secondary electrons (SE) and back scattered electrons (BSE).

The microstructures representative of F82H and 14YWT-SM6 in the unaffected region and/or HAZ are shown in Figure 6. The microstructure of F82H consisted of large prior austenite grain boundaries with fully martensitic lath structure as shown in Figure 6a. The microstructure of 14YWT-SM6 shown in Figure 6b consisted of <500 nm size grains that are nearly equiaxed in shape since the orientation of the polished specimen in normal to the extrusion axis.

(a)

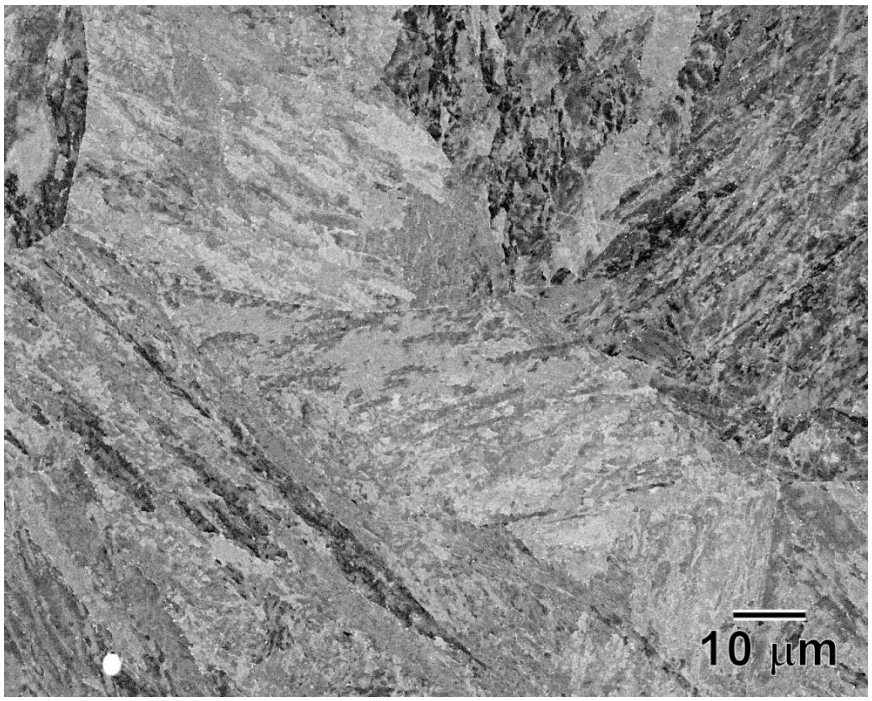

(b)

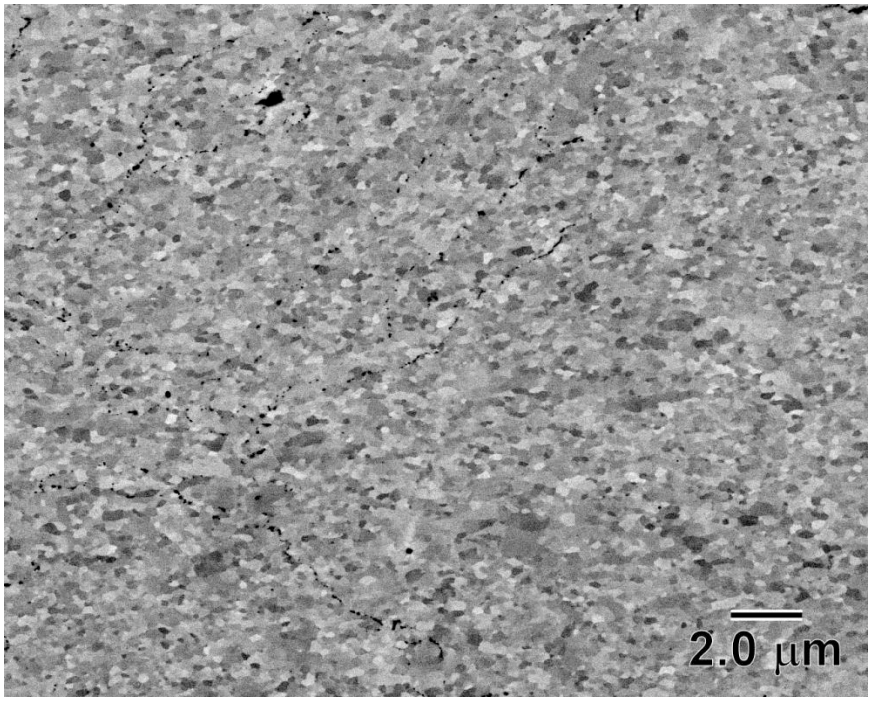

Figure 6. SEM backscattered electron micrographs showing the representative microstructures of (a) F82H and (b) 14YWT-SM6 in the unaffected or heat affected zones.

(a)

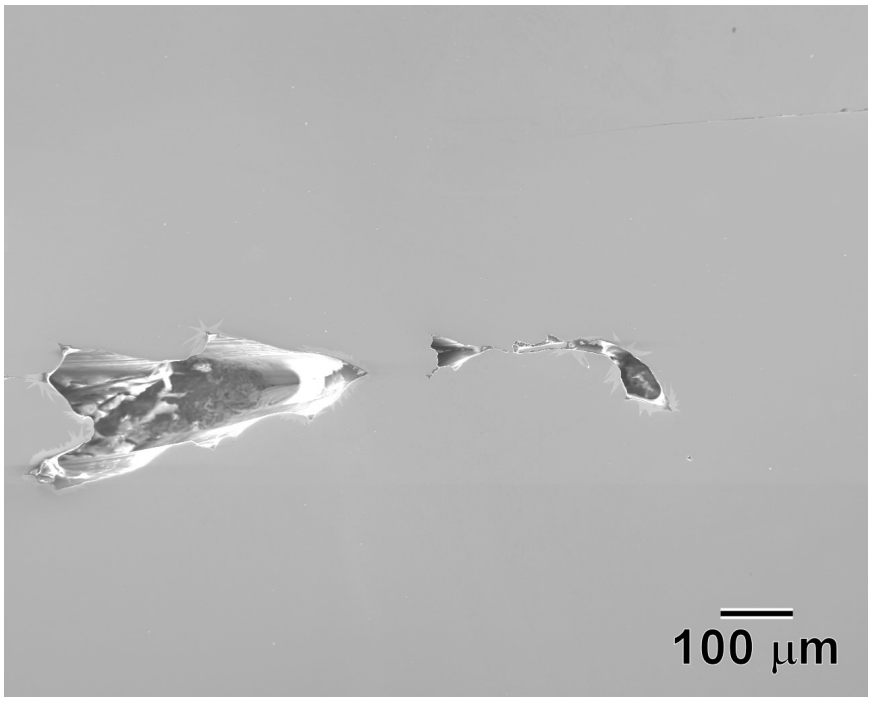

(b)

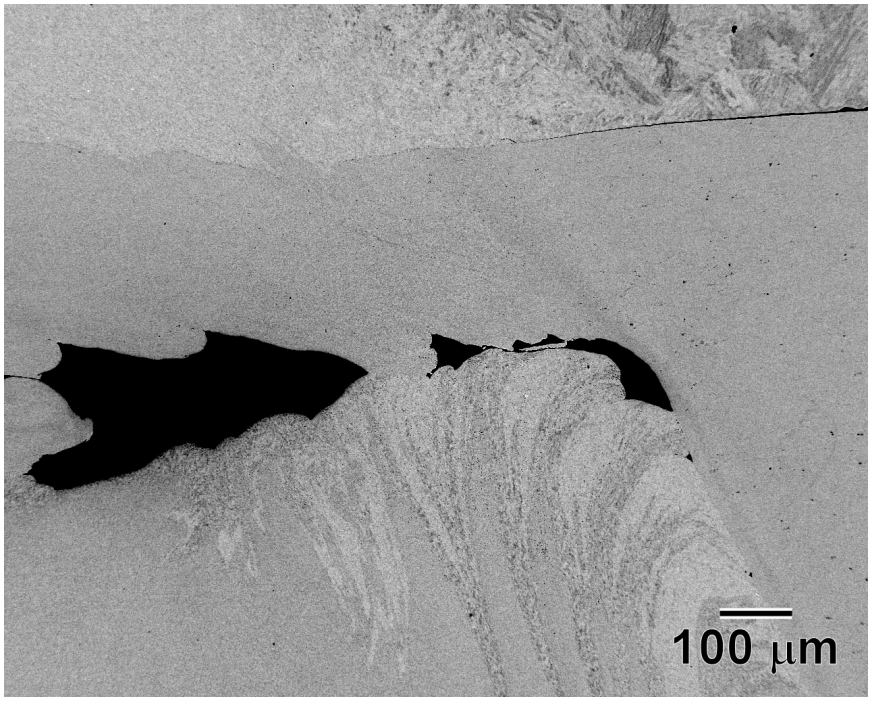

Figure 7. SEM micrographs showing the microstructure of F82H (top) and 14YWT-SM6 (bottom) near the large cavities that formed on the advancing side of the FSW zone. (a) secondary electron micrograph and (b) backscattered electron micrograph.

The microstructure that was observed by SEM near the large pores on the advancing side of the F82H/14YWT-SM6 specimen is shown in Figure 7 at a low magnification. The SE image in Figure 7a showed virtually no interfaces in the weld nugget and HAZ regions while the BSE image in Figure 7b revealed interfaces between F82H and 14YWT-SM6 in the top section of the weld nugget and between the TMAZ and HAZ of both F82H and 14YWT-SM6. The narrow gap between the unwelded F82H plate and 14YWT-SM6 specimen in the upper right region of the micrographs was observed to terminate at the weld zone. The BSE image in Figure 7b showed an extensive mixing pattern in the TMAZ located below the pores in 14YWT-SM6. This region pertained to the etched region observed above the pores by light microscopy in Figure 5. The BSE image also revealed a nonlinear interface between F82H and 14YWT-SM6 that provided evidence that mixing occurred between the two materials. The BSE image also indicated that considerable refinement in the microstructure occurred in the FSW nugget of F82H.

Coupled SE and BSE images of the interface observed between the TMAZ and HAZ of 14YWT-SM6 from the same location of the microstructure are shown at progressively higher magnifications in Figures 8 and 9, respectively. The bottom of the large pore located near the interface was included in these images to act as a reference point. The SE images observed in Figures 8a and 9a are sensitive to topographical features and revealed porosity in the TMAZ of 14YWT-SM6. The size and distribution of the pores were non-uniform, but were much smaller than the large pores present in the TMAZ. The BSE images shown in Figures 8b and 9b are sensitive to channeling effects related to grain orientation and allowed a more clear image of the grain size compared to the SE images. The BSE images showed that the interface region separating the TMAZ from the HAZ of 14YWT-SM6 was relatively narrow. The results indicated that FSW increased the grain size in the TMAZ by a factor of 2 to 4 times the size observed in the HAZ. This result implied that elevated temperatures greater than 1000ºC must have occurred during FSW based on results obtained from TMT processing of 14YWT that showed no increase in grain size after annealing at 1000ºC for 1 h. The analysis showed no correlation between the smaller pores and grain boundaries in the TMAZ. Although not fully understood, similar development of porosity has typically been observed on the advancing side of the FSZ joints in other studies [2].

The joint observed between F82H and 14YWT-SM6 in the weld nugget is shown in a set of coupled SE and BSE images recorded at progressively higher magnifications in Figures 10 and 11, respectively. At the lowest magnification shown in Figure 10, the SE and BSE images showed that good bonding occurred during FSW resulting in an interface between F82H and 14YWT-SM6. The BSE image in Figure 10b revealed that the interface was nonlinear due to mechanical mixing of the microstructures between F82H and 14YWT-SM6. However, no discernable grain structure can be observed in either F82H or 14YWT-SM6 at the low magnification. At the higher magnification shown in Figure 11, extensive porosity was observed to have developed at the interface between F82H and 14YWT-SM6 during FSW. The analysis indicated that the size and distribution of the pores was non-uniform and that there was no correlation between these pores and the grain boundaries in the TMAZ of F82H and 14YWT-SM6. It should be noted that the white features observed by SE in Figure 11a are colloidal silica particles used for the final polishing of the specimen that were not completed removed during cleaning. The BSE image in Figure 11b showed that the interface region separating the TMAZ of F82H and 14YWT-SM6 was relatively narrow. However, the FSW decreased the grain size in the TMAZ of F82H that resulted in equiaxed morphology and modified martensitic lath structure. In the TMAZ of 14YWT-SM6, the FSW increased the grain size and appeared to have slightly elongated the grains with an orientation relative to the interface. Additional SE and BSE images were recorded along the joint between F82H and 14YWt-SM6 and the results showed that porosity was present along the entire joint. The origin of the porosity may be

related to the narrow gap that existed between the F82H plate and the bend bar specimens of 14YWT-SM6 that was mixed and redistributed into pores during the solid state mechanical mixing.

(a)

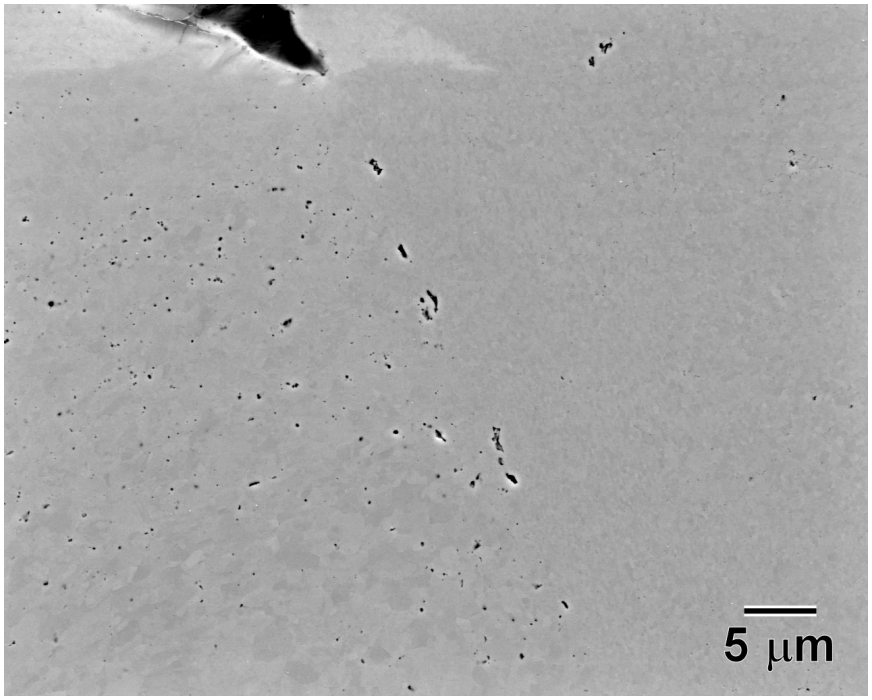

(b)

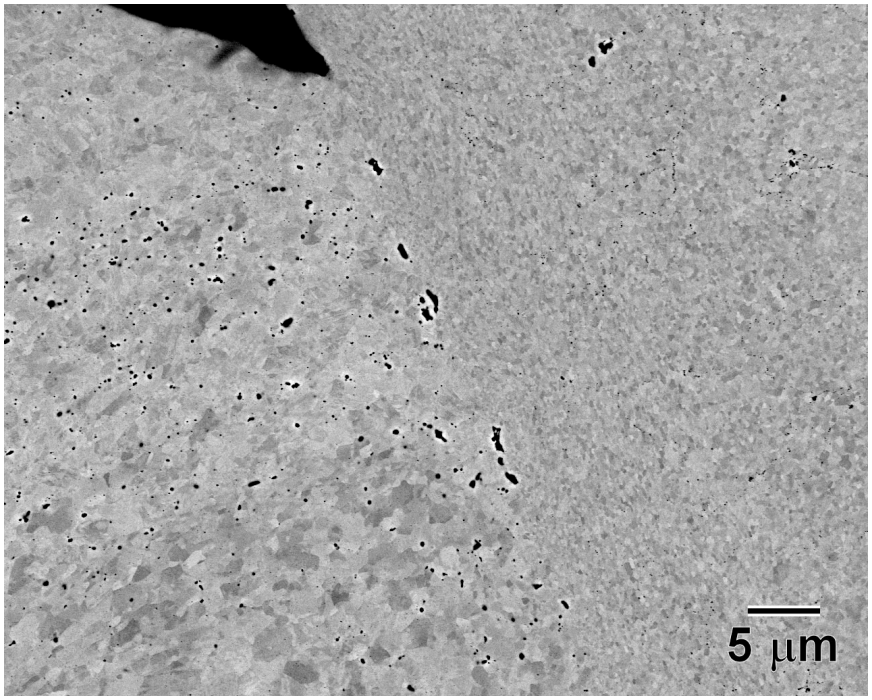

Figure 8. SEM micrographs of the joint between the FSW zone (left) and unaffected microstructure (right) of 14YWT-SM6. (a) Secondary electron micrograph and (b) backscattered electron micrograph.

(a)

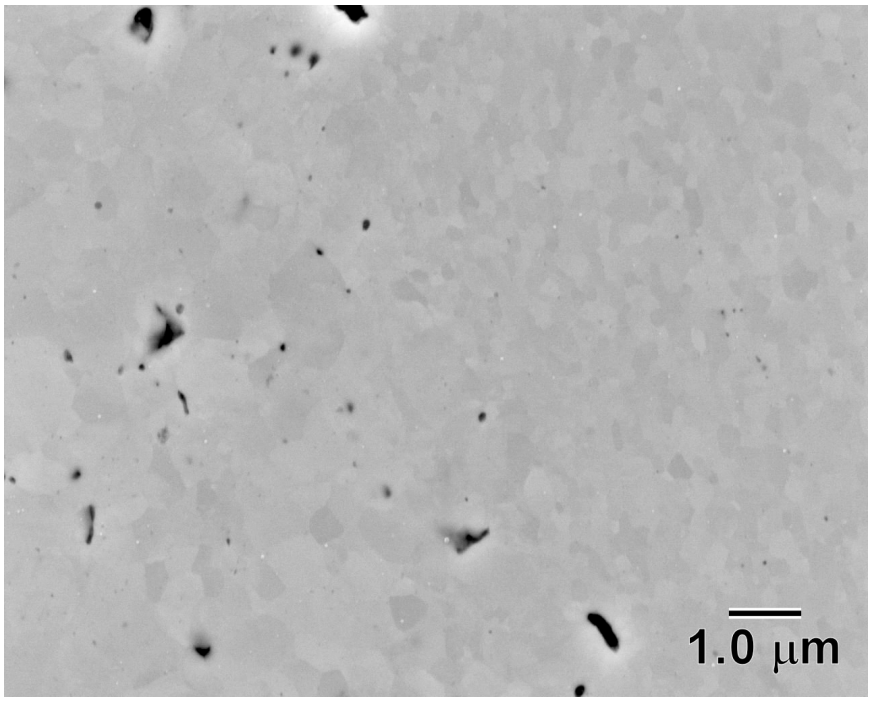

(b)

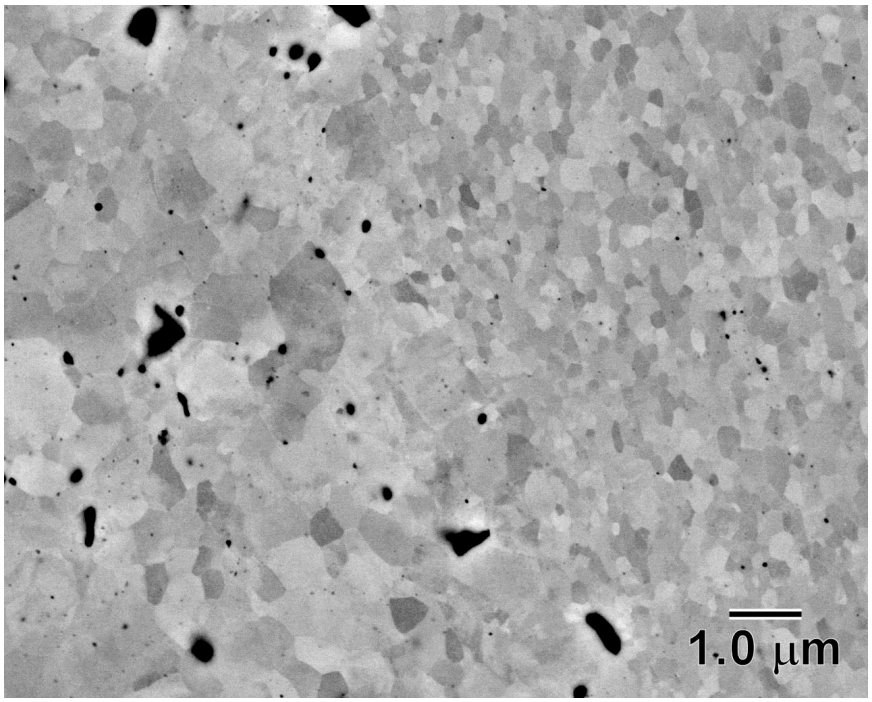

Figure 9. High magnification SEM micrographs of the joint between the FSW zone (left) and unaffected microstructure (right) of 14YWT-SM6. (a) Secondary electron micrograph and (b) backscattered electron micrograph.

(a)

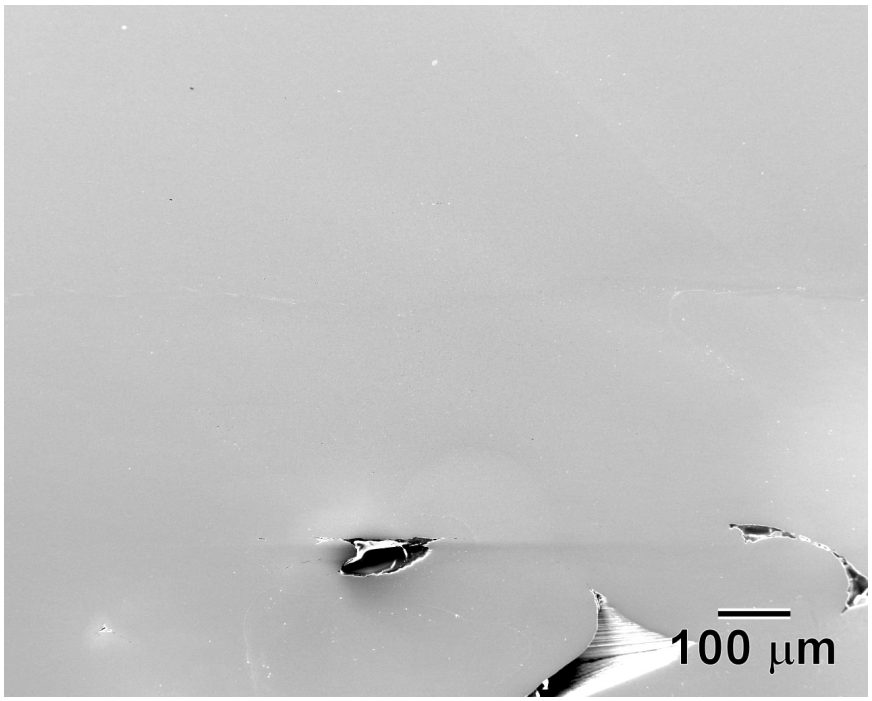

(b)

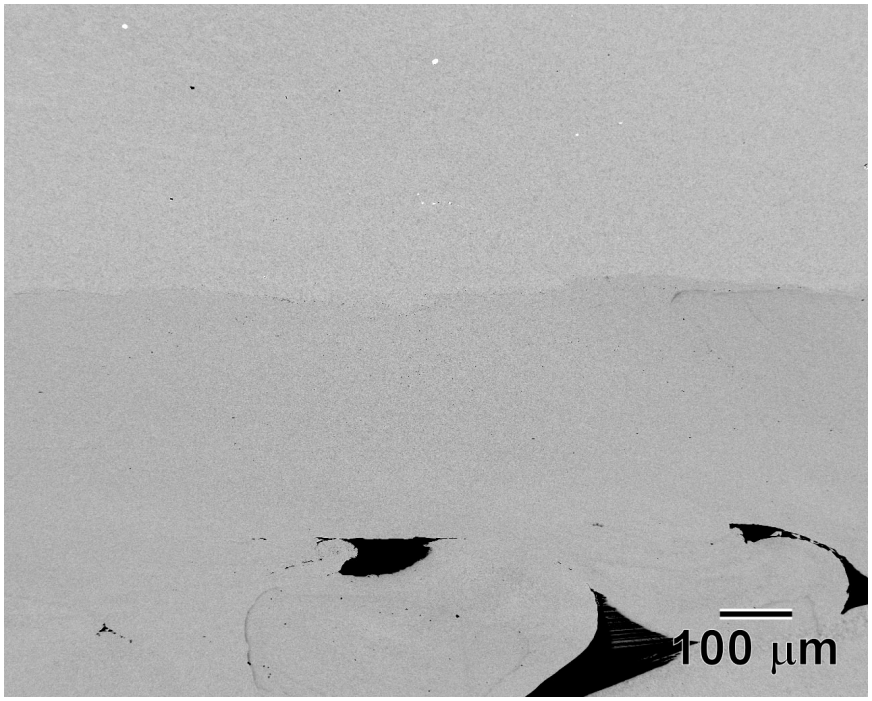

Figure 10. SEM micrographs showing the joint between the FSW zones of F82H (top) and 14YWT-SM6 (bottom) and the large cavities in the FSW zone of 14YWT-SM6. (a) Secondary electron micrograph and (b) backscattered electron micrograph.

(a)

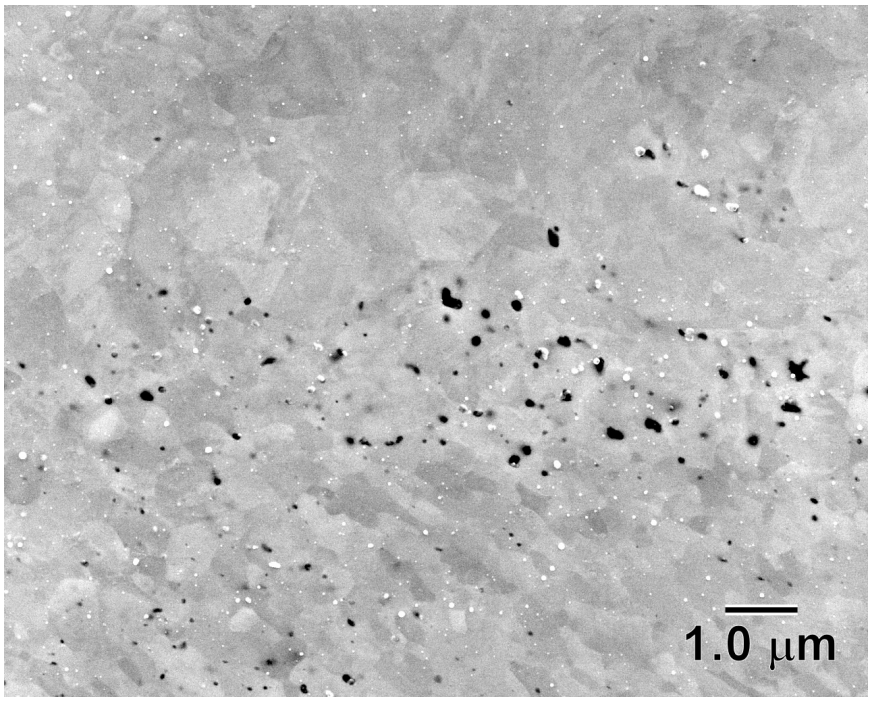

(b)

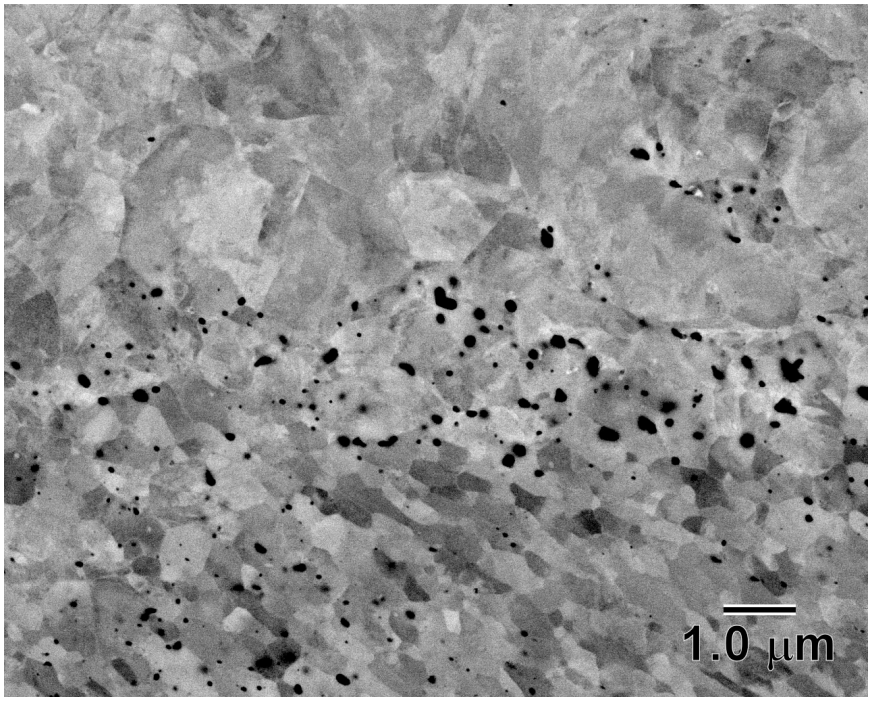

Figure 11. SEM micrographs of the joint between the FSW zones of F82H (top) and 14YWT-SM6 (bottom). (a) Secondary electron micrograph and (b) backscattered electron micrograph.

No results have been obtained on the microstructural characterization of the interfaces between the TMAZ and HAZ on the retreating side of the 14YWT-SM6 specimen or near the center where the joint between 2 bend bar specimens of 14YWT-SM6 is present. These regions will be characterized in the near future.

CONCLUSION

The initial attempt to join bend bar specimens of the advanced ODS 14YWT-SM6 alloy to each other and 14YWT-SM6 specimens to F82H plate was successfully obtained by friction stir welding. The joints were characterized by light microscopy and SEM analysis showed overall good bonding between TMAZ and HAZ of 14YWT-SM6 and between F82H and 14YWT-SM6. The interfaces were observed to be relatively narrow in width. However, porosity was observed in the TMAZ of 14YWT-SM6 on the advancing side of the FSW joint and at the interface between F82H and 14YWT-SM6. Further refinements in the FSW process will be required to minimize defects including porosity.

FUTURE WORK

The next procedure for characterization of the FSW joints present in the F82H/14YWT-SM6 sample will involve the preparation of TEM specimens using the lift-out procedure from strategic locations in the polished specimen and thinning by the Focused Ion Beam (FIB) method. The purpose of the TEM analysis will be to investigate the effect that FSW had on the size and distribution (spatial and number density) of the Ti-, Y- and O-enriched nanoclusters present in 14YWT-SM6 and to study the mixing characteristics of the microstructures between F82H and 14YWT-SM6 at the interface.

REFERENCES

[1] W. M. Thomas, E. D Nicholas, J. C. Needham, M. G. Murch, P. Templesmith and C. J. Dawes, G. B. Patent Application No. 9125978.8, 1991.
[2] R. S. Mishra and Z. Y. Ma, *Mater. Sci. Eng. R* **50** (2005) 1-78.
[3] S. M. Howard, B. K. Jasthi, W. J. Arbegast, G. J. Grant, S. Koduri, D. R. Herling and D. S. Gelles, DOE/ER-0313/37, 2004, 55-60.
[4] P. Miao, G. R. Odette, J. Gould, J. Bernath, R. Miller, M. Alinger, and C. Zanis, *J. Nucl. Mater.* **367–370** (2007) 1197-1202.
[5] Z. Feng and W. Ren, **Initial Development in Joining of ODS Alloys Using Friction Stir Welding**, ORNL/GEN4/LTR-06-021, (2006).
[6] Z. Feng and W. Ren, 2007 ASME PVP Conference, paper number PVP200726663.
[7] G. J. Grant, D. S. Gelles, R. J. Steel and R. Lindau, DOE/ER-0313/38 (2005) 47-53.
[8] F. Legendre, S. Poissonnet, P. Bonnaillie, L. Boulanger and L. Forest, *J. Nucl. Mater.* **386-388** (2009) 537-539.
[9] D. T. Hoelzer, J. Bentley, M. A. Sokolov, M. K. Miller, G. R. Odette and M. J. Alinger, *J. Nucl. Mater.* **367-370** (2007) 166-172.
[10] D. A. McClintock, Ph.D. Dissertation, Univ. of Texas, Austin (2008).
[11] D. A. McClintock, D. T. Hoelzer, M. A. Sokolov and R. K. Nanstad, *J. Nucl. Mater.* **386–388** (2009) 307–311.
[12] D. A. McClintock, M. A. Sokolov, D. T. Hoelzer and R. K. Nanstad, *J. Nucl. Mater.* **392** (2009) P353–359.